Available online at www.sciencedirect.com

SciVerse ScienceDirect

Ceramics International 38 (2012) 2277–2282

CERAMICS INTERNATIONAL

www.elsevier.com/locate/ceramint

Microstructure and electrical properties of relaxor $(1-x)[(K_{0.5}Na_{0.5})_{0.95}Li_{0.05}](Nb_{0.95}Sb_{0.05})O_3$–$xBaTiO_3$ piezoelectric ceramics

Wenjuan Wu, Dingquan Xiao *, Jiagang Wu, Jing Li, Jianguo Zhu, Bin Zhang

Department of Materials Science, Sichuan University, Chengdu 610064, PR China

Received 2 September 2011; received in revised form 18 October 2011; accepted 27 October 2011
Available online 4 November 2011

Abstract

In order to solve the low temperature stability of electrical properties in KNN-based ceramics, $(1-x)[(K_{0.5}Na_{0.5})_{0.95}Li_{0.05}](Nb_{0.95}Sb_{0.05})O_3$–$xBaTiO_3$ [$(1-x)$KNLNS–xBT] lead-free piezoelectric ceramics were prepared by the conventional solid-state sintering method. The introduction of BT stabilizes the tetragonal phase of KNLNS ceramics at room temperature, results in a typical ferroelectric relaxor behavior, and shifts the polymorphic phase transition to below room temperature. Moreover, there is a strong $BaTiO_3$ concentration dependence of relaxor behavior and electrical properties, and the ceramic with $x = 0.005$ exhibits optimum electrical properties and typical relaxor behavior ($d_{33} = 269$ pC/N, $k_p = 0.50$, $\varepsilon_r = 1371$, $\tan\delta = 0.03$, $T_C \sim 349$ °C and $\gamma = 1.88024$). These results indicate that the BT is an effective way to improve the temperature stability as well as the electrical properties of KNN-based ceramics.

Keywords: C. Electrical properties; $(K_{0.5}Na_{0.5})NbO_3$; $BaTiO_3$; Lead-free piezoelectric ceramics; Ferroelectric relaxor

1. Introduction

Considerable attention for lead-free piezoelectric ceramics has been recently given to $(K_{0.50}Na_{0.50})NbO_3$ (KNN)-based ceramics, due to their excellent electrical properties, a high Curie temperature, and environmental friendliness [1–16]. These experimental results show that KNN-based lead-free ceramics exhibit arguable, comparable piezoelectric properties to conventional $Pb(Zr,Ti)O_3$ ceramics because of an orthorhombic to tetragonal (O–T) polymorphic phase transition (PPT) occurring near room temperature [2–5,11]. In contrast, this phase transition also correspondingly results in a strong temperature dependence of dielectric and piezoelectric properties, thus limiting the practical application of the KNN-based piezoelectric ceramics [3–5,11]. Recently, some attempts have been conducted on KNN-based solid solutions with $CaTiO_3$ (CT) for improving the temperature stability by decreasing the PPT, but their piezoelectric properties are not still ideal [3–5,11]. Therefore, the improvement in the temperature stability and piezoelectric properties of KNN-based ceramics currently becomes a tough issue for the practical application in the field of piezoelectric materials.

In the present work, we choose $BaTiO_3$ (BT) to dope KNN-based ceramics in order to decrease the O–T PPT to below room temperature. On introducing BT to KNN-based ceramics, there exists a valence mismatch both in the perovskite A-site and B-site, and the O–T polymorphic phase transition toward room temperature which seem to have a firm relation with the perovskite B-site ions [17,18]. The BT is suitable for the development of temperature stability. As our previous research reports [19], the lead-free ferroelectrics with a composition of 0.995KNLNS–$0.005BaTiO_3$ ceramic exhibits a typical ferroelectric relaxor behavior, that is, the dielectric peaks become increasingly broader, and the temperature of the maximum dielectric constant is shifted to a higher temperature with increasing frequencies. The dielectric relaxor behavior follows the modified Curie–Weiss law [19]. However, the investigations on the effect of BT content on the electric and relaxor properties of KNN-based were not detailed and exhaustive. Therefore, $(1-x)[(K_{0.5}Na_{0.5})_{0.95}Li_{0.05}](Nb_{0.95}Sb_{0.05})O_3$–$xBaTiO_3$

* Corresponding author.
E-mail address: nic0402@scu.edu.cn (D. Xiao).

0272-8842/$36.00
doi:10.1016/j.ceramint.2011.10.079

[(1 − x)KNLNS–xBT] lead-free ceramics were prepared. The effect of the BT addition on the microstructure, relaxor behavior, and electrical properties of (1 − x)KNLNS–xBT ceramics were systematically studied, and the underlying physical mechanisms were investigated.

2. Experimental

$(1-x)[(K_{0.5}Na_{0.5})_{0.95}Li_{0.05}](Nb_{0.95}Sb_{0.05})O_3$–$xBaTiO_3$ [(1 − x)KNLNS–xBT] (x = 0.0025, 0.005, 0.01, 0.015, 0.02 and 0.03, respectively) ceramics were prepared by the conventional solid state reaction fabrication technique. K_2CO_3 (99%), Na_2CO_3 (99.8%), Li_2CO_3 (99.99%), Nb_2O_5 (99.5%), Sb_2O_3 (98%), $BaCO_3$ (99%), and TiO_2 (99.99%) were used as starting raw materials. Stoichiometric powders were mixed by the ball milling for 24 h with the zirconia balls media in anhydrous ethanol and then dried, and these dried powders were calcined at 850 °C for 6 h. These calcined powders were pressed into disks at 20 MPa using polyvinyl alcohol (PVA) as a binder with diameters of ∼15 mm and thicknesses of ∼1.1–1.3 mm. After burning off PVA, these ceramic disks were sintered in the temperature range of 1090–1150 °C for 2–3 h in air. These specimens were poled in a silicon oil bath at 30 °C by applying a dc electric field of 3–4 kV/mm for 30 min. All electrical measurements were conducted on aged specimens (24 h after poling).

The phase structure of these specimens was examined by the X-ray diffraction (XRD) using Cu Kα radiation (λ = 1.54178 Å) in the θ–2θ scan mode (DX1000, Dandong, China). Surface morphologies of sintered specimens were observed by a scanning electron microscope (SEM) (JSM-5900, Japan). The density of sintered samples was determined by the Archimedes method. Silver paste was sintered on both sides of the specimens at 700 °C for 10 min to form electrodes for the dielectric and piezoelectric measurements. Their piezoelectric constant (d_{33}) was measured using a piezo-d_{33} meter (ZJ-3A, China). The dielectric constant as a function of temperature of these ceramics was obtained by using an *LCR* meter (HP 4980, Agilent, U.S.A.).

3. Results and discussion

Fig. 1(a) shows the XRD patterns of (1 − x)KNLNS–xBT ceramics as a function of x (x = 0.0025, 0.005, 0.01, 0.015, 0.02 and 0.03, respectively). (1 − x)KNLNS–xBT ceramics with $x \leq 0.015$ are of a single-phase perovskite structure, and no secondary phases were observed in the range detected. For these (1 − x)KNLNS–xBT ceramics with $x > 0.015$, a small amount of the secondary phase ($Ba_6Ti_2Nb_8O_{30}$) were formed due to too high sintering temperature, and these secondary phases are related to the volatilization of Na_2O at a high sintering temperature [20]. Therefore, a small amount of BT can easily enter into the KNLNS lattice to form a stable (1 − x)KNLNS–xBT solid solution. Fig. 1(b) plots the enlarged XRD patterns of (1 − x)KNLNS–xBT ceramics in the range of 2θ from 42° to 48°. It can be observed that the room-temperature phase structure of all (1 − x)KNLNS–xBT ceramics belongs to a tetragonal phase, whereas the temperature dependence of the dielectric constant (Fig. 5) also confirms that there is no coexistence of two phases at a room temperature. Moreover, it is of interest to note that the diffraction peaks slightly shift toward a higher diffraction angle as x increases. Fig. 2 shows the variation in lattice parameters as a function of x. The tetragonality (c/a ratio) of (1 − x)KNLNS–xBT ceramics decreases with the increase of x. It could be concluded that the BT addition results in the lattice distortion of (1 − x)KNLNS–xBT ceramics which is well in agreement with the peak shifts in Fig. 1.

Surface morphologies of (1 − x)KNLNS–xBT ceramics with x = 0.0025, 0.005, 0.01, 0.015, 0.02 and 0.03 are shown in

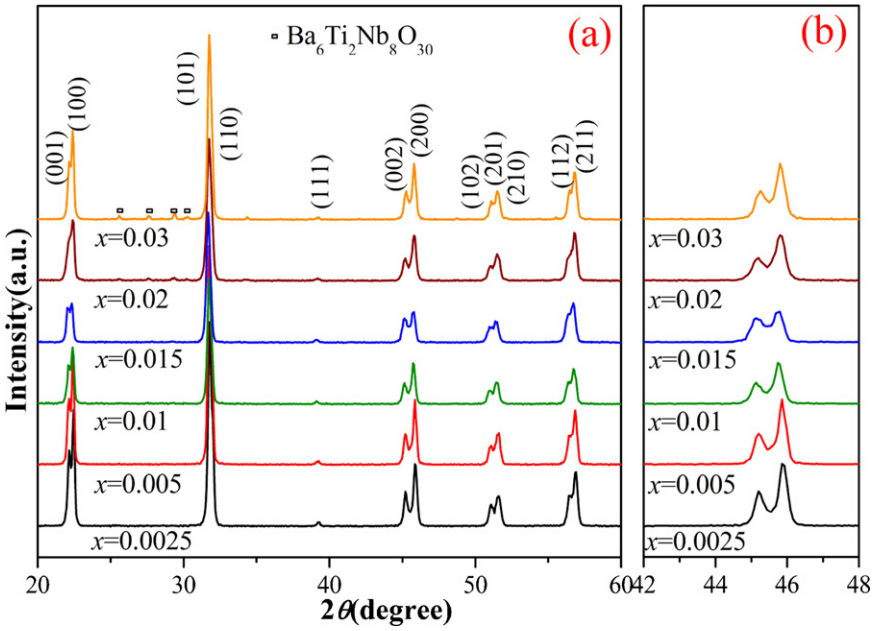

Fig. 1. (a) XRD patterns of (1 − x)KNLNS–xBT ceramics. (b) Enlarged XRD patterns of (1 − x)KNLNS–xBT ceramics in the range of 2θ from 42° to 48°.

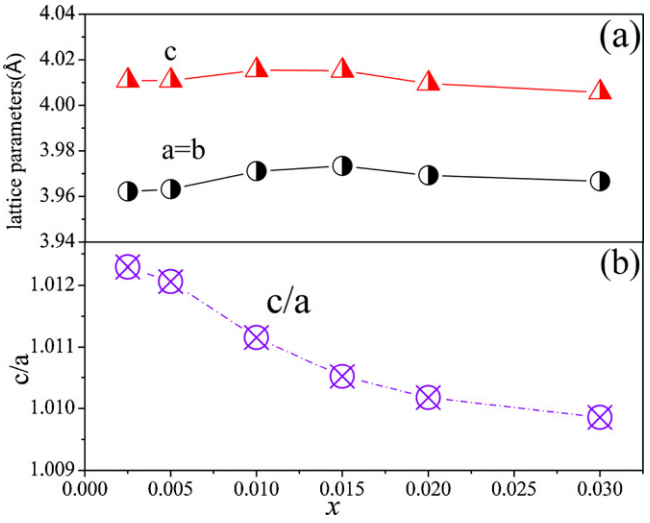

Fig. 2. (a) Lattice parameters and (b) c/a of $(1-x)$KNLNS–xBT ceramics as a function of x.

Fig. 3(a)–(f), respectively. All ceramics have a dense microstructure, and the grains exhibit usually rectangular in shape. Moreover, the average grain size of the $(1-x)$KNLNS–xBT ceramics slowly decreases from ~3.2 μm to ~1.9 μm with the increase of the BT content at $x \leq 0.015$, and then dramatically decreases to ~1 μm with the further increase of the BT content. This could be attributed to a big difference between the ionic radius of Ba^{2+} (135 pm) and Na^{+} (102 pm) and the possibility that Ba^{2+} aggregates and the secondary phase on a very small scale at these grain boundaries. A small grain size may prevent the movement of the grain boundary, and thus may affect the electrical properties of $(1-x)$KNLNS–xBT ceramics.

Fig. 4 shows the densities ρ of $(1-x)$KNLNS–xBT ceramics as a function of x. The ρ of these ceramics increases with the increase of x from 0.0025 to 0.005, and keeps almost unchanged at $x = 0.005$–0.015, indicating that the BT addition is an effective method in promoting the densification of KNN-based ceramics.

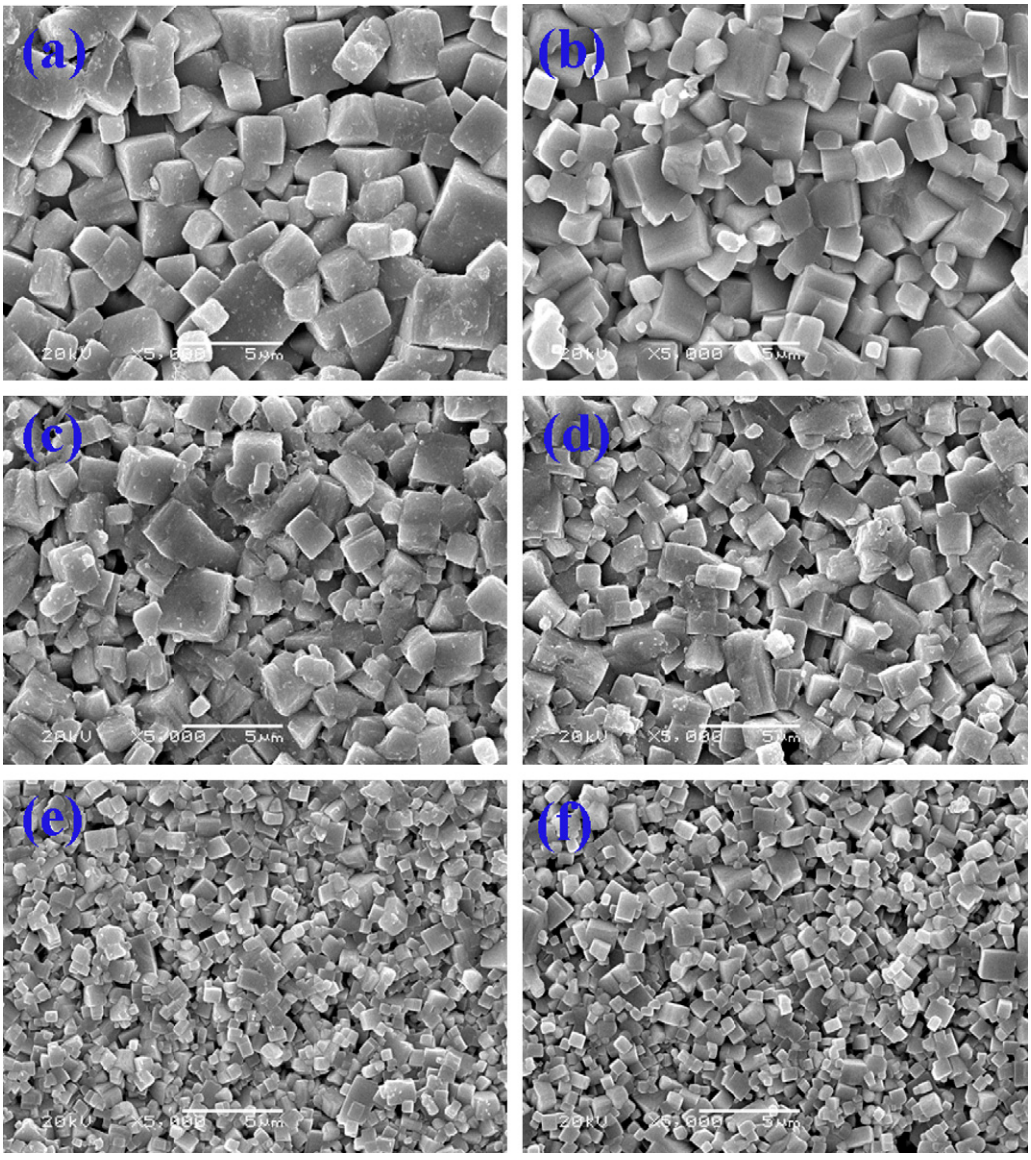

Fig. 3. SEM patterns of $(1-x)$KNLNS–xBT ceramics as a function of x. (a) $x = 0.0025$, (b) $x = 0.005$, (c) $x = 0.01$, (d) $x = 0.015$, (e) $x = 0.02$, and (f) $x = 0.03$.

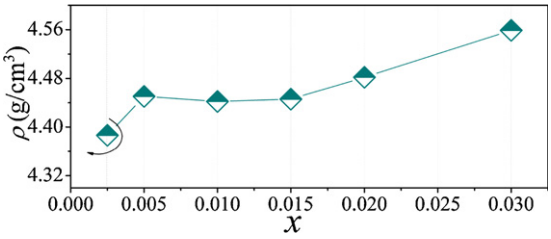

Fig. 4. Densities ρ of $(1-x)$KNLNS–xBT ceramics as a function of x.

Especially, the density abruptly increases with $x > 0.015$ due to the formation of the secondary phase. The high density also matches with the dense microstructure in Fig. 3.

The temperature dependence of the dielectric constant (ε_r) for the $(1-x)$KNLNS–xBT ceramics ($x = 0.0025$, 0.005, 0.01, 0.015, 0.02 and 0.03, respectively) measured at 10 kHz is shown in Fig. 5. A tetragonal–cubic phase transition (T_C) is observed in the $(1-x)$KNLNS–xBT ceramics, while a orthorhombic–tetragonal phase transition (T_{o-t}) cannot be observed in the temperature range involved. This result confirms that the T_{o-t} of $(1-x)$KNLNS–xBT ceramics shifts to below room temperature, indicating its tetragonal structure at room temperature, which is in agreement with the XRD results (Fig. 1). Usually, the T_{o-t} locating at below room temperature benefits the temperature stability of KNN-based ceramics [3,5,11]. Fig. 6 plots the T_C of $(1-x)$KNLNS–xBT ceramics as a function of x. The observed T_C of these ceramics decreases from ~361 °C to ~270 °C with the increase of x due to the introduction of BT with a lower Curie temperature. However, the Curie temperature ($T_C \sim 349$ °C) of 0.995KNLNS–0.005BT ceramics slightly decreases.

It is of great interest to note that the dielectric peaks at T_C for all ceramics are relatively broad, indicating the characteristic of the diffuse phase transition from tetragonal phase to cubic phase. The diffuseness of the phase transition can be described

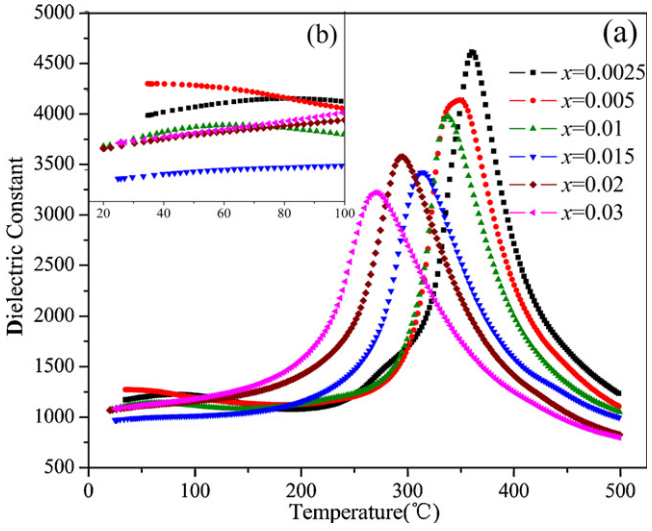

Fig. 5. Temperature dependence of the ε_r for $(1-x)$KNLNS–xBT ceramics at 10 kHz as a function of x.

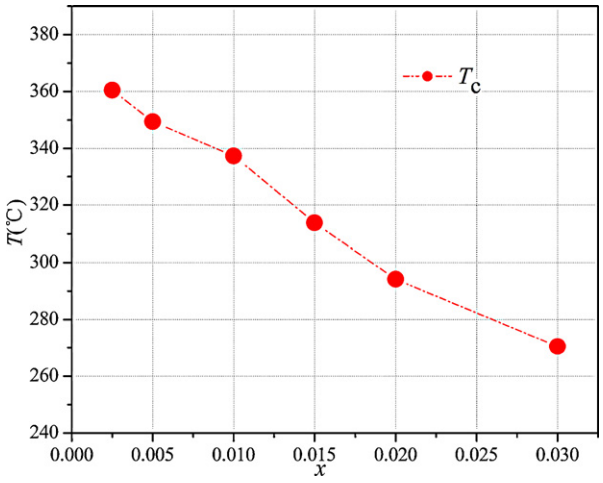

Fig. 6. T_c of $(1-x)$KNLNS–xBT ceramics as a function of x.

by the modified Curie–Weiss law [21],

$$\frac{1}{\varepsilon_r} - \frac{1}{\varepsilon_m} = C^{-1}(T - T_m)\gamma \quad (1)$$

where the ε_m is the maximum value of ε_r at the phase transition temperature T_m, the γ is the degree of the diffuseness, and the C is the Curie-like constant. The γ has a value ranging from 1 for a normal ferroelectric to 2 for an ideal relaxor ferroelectric. Fig. 7(a)–(f) shows the plots of $\ln(1/\varepsilon_r - 1/\varepsilon_m)$ vs $\ln(T - T_m)$ for the $(1-x)$KNLNS–xBT ceramics with $x = 0.0025$, 0.005, 0.01, 0.015, 0.02 and 0.03, respectively. All ceramics exhibit a linear relationship in the plots of $\ln(1/\varepsilon_r - 1/\varepsilon_m)$ vs $\ln(T - T_m)$. Fig. 8 shows the γ value of $(1-x)$KNLNS–xBT ceramics as a function of x, where the γ value was determined by the least-squared fitting the experimental data to the equation. The γ value reaches a maximum of ~1.88024 at $x = 0.005$, confirming that these $(1-x)$KNLNS–xBT ceramics are of relaxor ferroelectrics. In contrast to normal ferroelectrics, dynamic polar nanometer-sized regions (PNRs) appear in relaxor ferroelectrics. The local electric fields and elastic fields give rise to the PNRs, by hindering the long-range dipole alignment. For these $(1-x)$KNLNS–xBT ceramics, Na^+, K^+, and Ba^{2+} locate at the A-sites and Ti^{4+} and Nb^{5+} locate at the B-sites of the ABO_3 perovskite structure. Ba^{2+} has different valence and ionic radii as compared with Na^+ and K^+, resulting in the formation of the local electric fields due to the local charge imbalance and local elastic fields caused by the local structure distortions. The similar phenomenon also occurs at the B site in $(1-x)$KNLNS–xBT ceramics. Therefore, the relaxor behavior in $(1-x)$KNLNS–xBT ceramics should be attributed to the cationic disorder induced by both A-sites and B-sites substitutions. However, the local electric fields and elastic fields could interact; namely, the random fields may decrease owing to the interaction between the local electric fields and elastic fields. Therefore, the degree of the relaxor behavior reaches the maximum at $x = 0.005$ in $(1-x)$KNLNS–xBT ceramics [22–24].

Fig. 9 shows the dielectric properties (ε_r and $\tan\delta$) as a function of x for the $(1-x)$KNLNS–xBT ceramics, measured

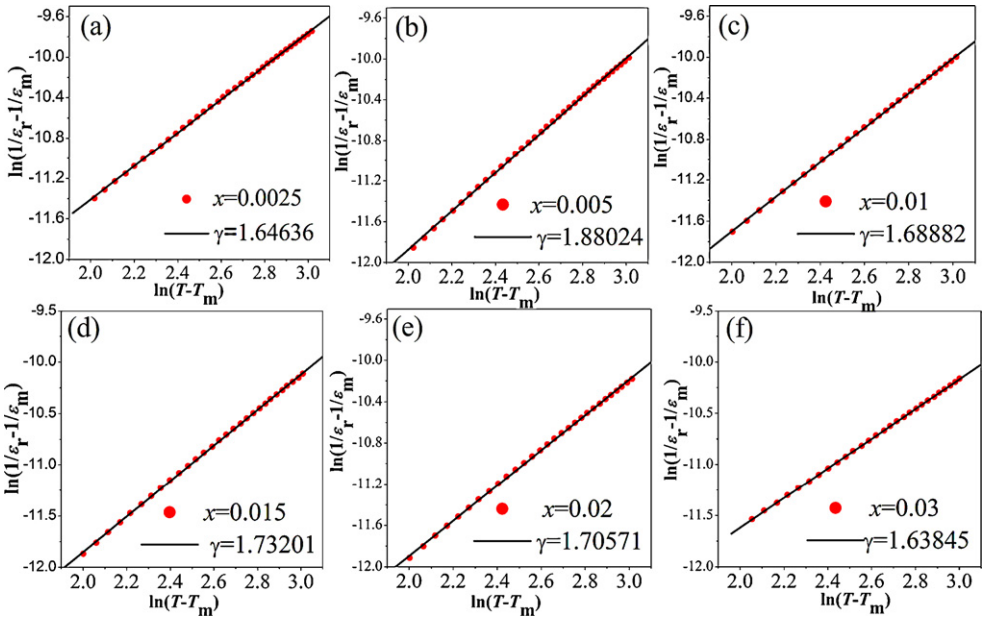

Fig. 7. Plots of $\ln(1/\varepsilon_r - 1/\varepsilon_m)$ vs $\ln(T - T_m)$ at 10 kHz for the $(1-x)$KNLNS–xBT ceramics with $x = 0.0025$, 0.005, 0.01, 0.015, 0.02 and 0.03, respectively. The symbols denote experimental data while the solid lines denote the linear fitting line to the equation.

at room temperature. The $(1-x)$KNLNS–xBT ceramic at $x = 0.005$ exhibits a higher dielectric constant ($\varepsilon_r = 1371$) and a lower dielectric loss ($\tan\delta = 0.03$) at room temperature as compared with those of these ceramics with other components. This phenomenon may be explained that the high phase purity and good microstructure result in the improvement of dielectric properties of the ceramic at $x = 0.005$; at a higher BT content, the formation of second phase degrades the dielectric properties of the ceramics.

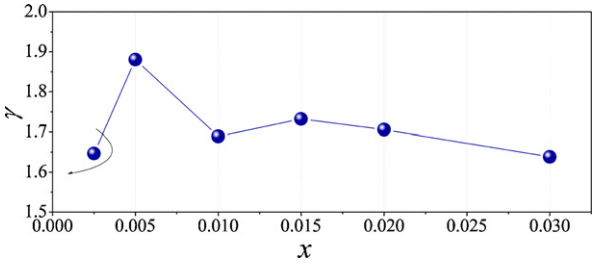

Fig. 8. γ of $(1-x)$KNLNS–xBT ceramics as a function of x.

Fig. 10 shows the dependence of the piezoelectric coefficient (d_{33}) and electromechanical coupling factor (k_p) of $(1-x)$KNLNS–xBT ceramics on x. The d_{33} value increases with the increase of x, reaches a maximum value ($d_{33} \sim 269$ pC/N) at $x = 0.005$, and then decreases with further increasing x. Similarly to the change of d_{33}, the k_p also reaches a maximum value of ~0.50 at $x = 0.005$. These results indicate that these $(1-x)$KNLNS–xBT ceramics with $x = 0.005$ possess optimum piezoelectric properties at room temperature. Usually, the KNN-based lead-free materials exhibit excellent piezoelectric properties owing to an orthorhombic to tetragonal

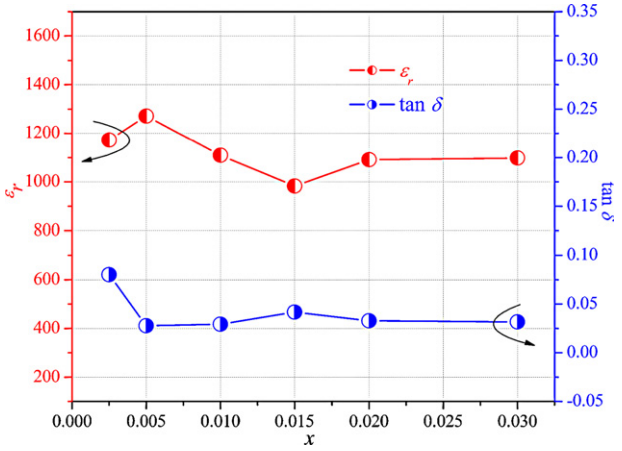

Fig. 9. Dielectric properties for the $(1-x)$KNLNS–xBT ceramics as a function of x.

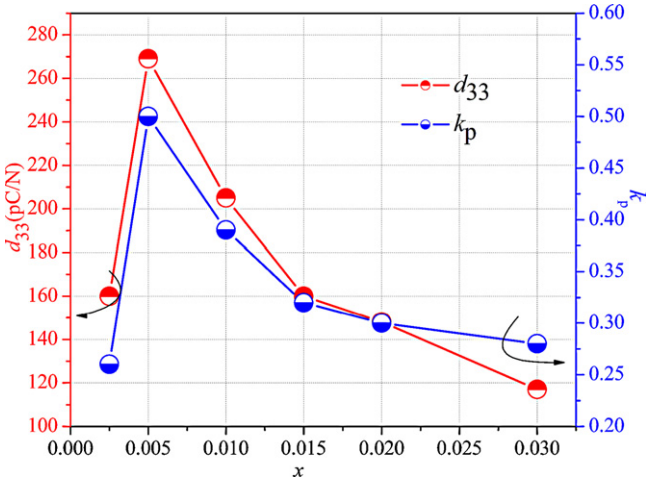

Fig. 10. Piezoelectric properties of the $(1-x)$KNLNS–xBT ceramics as a function of x.

polymorphic phase transition (T_{o-t}) occurring near room temperature. However, the T_{o-t} of these $(1-x)$KNLNS–xBT ceramics with $x = 0.005$ was shifted to below room temperature (Figs. 1 and 3). As a result, good piezoelectric properties at room temperature should be attributed to an optimum $BaTiO_3$ content, where the optimum lattice distortion and the dense microstructure are also induced for the 0.995KNLNS–0.005BT ceramics. Similar phenomenon was also observed for these $CaTiO_3$-modified KNN-based ceramics [3,5]. The $CaTiO_3$ helps improve the temperature stability of KNN-based ceramics, but their piezoelectric properties ($d_{33} \sim 210$ pC/N) were degraded [3]. In the present work, the piezoelectric constant of BT-modified KNLNS ceramics is superior to those of CT-modified KNLNS ceramics reported by other authors. Therefore, the BT is a better way to solve the temperature stability of KNN-based ceramics, which benefits the development of KNN-based ceramics.

4. Conclusions

Effects of the $BaTiO_3$ addition on the microstructure, relaxor behavior, piezoelectric and dielectric properties of $(1-x)[(K_{0.5}Na_{0.5})_{0.95}Li_{0.05}](Nb_{0.95}Sb_{0.05})O_3$–$x$$BaTiO_3$ ($x = 0.25$–3 mol%) [$(1-x)$KNLNS–xBT] piezoelectric ceramics were systematically studied. These $(1-x)$KNLNS–xBT ceramics are of a typical ferroelectric relaxor behavior. The addition of $BaTiO_3$ in KNLNS materials shifts the T_{o-t} to be below room temperature, indicating that the introduction of $BaTiO_3$ stabilizes the tetragonal phase of KNLNS materials at room temperature. $(1-x)$KNLNS–xBT ($x = 0.005$) piezoelectric ceramics with a typical ferroelectric relaxor behavior possess optimum properties of $d_{33} = 269$ pC/N, $k_p = 0.50$, $\varepsilon_r = 1371$, $\tan\delta = 0.03$, and $T_C \sim 349$ °C. Therefore, the BT is a better way to solve the temperature stability of KNN-based ceramics, which benefits the development of KNN-based ceramics.

Acknowledgements

This work was supported by National Science Foundation of China (NSFC Nos. 50772068, 50972001, and 51102173), the supports of the introduction of talent start funds of Sichuan University (2082204144033), and Foundation of Doctor Training Program in University and College in China (Nos. 20030610035 and 20080610020). Thank reviewers and editor for their good comments and advice, which benefits to the improvement of our paper.

References

[1] L. Egerton, D.M. Dillom, Piezoelectric and dielectric properties of ceramics in the system potassium–sodium niobate, J. Am. Ceram. Soc. 42 (1959) 438–442.

[2] Y. Saito, H. Takao, T. Tani, T. Nonoyama, K. Takatori, T. Homma, T. Nagaya, M. Nakamura, Lead-free piezoceramics, Nature 432 (2004) 84–87.

[3] S.J. Zhang, R. Xia, T.R. Shrout, Modified $(K_{0.5}Na_{0.5})NbO_3$ based lead-free piezoelectrics with broad temperature usage range, Appl. Phys. Lett. 91 (2007) 132913-1–132913-3.

[4] S.J. Zhang, R. Xia, T.R. Shrout, G.Z. Zang, J.F. Wang, Characterization of lead free $(K_{0.5}Na_{0.5})NbO_3$–$LiSbO_3$ piezoceramic, Solid. State Commun. 141 (2007) 675–679.

[5] J.G. Wu, D.Q. Xiao, Y.Y. Wang, W.J. Wu, B. Zhang, J. Li, J.G. Zhu, $CaTiO_3$-modified $[(K_{0.5}Na_{0.5})_{0.94}Li_{0.06}](Nb_{0.94}Sb)O_3$ lead-free piezoelectric ceramics with improved temperature stability, Scripta Mater. 59 (2008) 750–752.

[6] Y. Guo, K. Kakimoto, H. Ohsato, Phase transitional behavior and piezoelectric properties of $(Na_{0.5}K_{0.5})NbO_3$–$LiNbO_3$ ceramics, Appl. Phys. Lett. 85 (2004) 4121–4123.

[7] M. Matsubara, T. Yamaguchi, W. Sakamoto, K. Kikuta, T. Yogo, S. Hirano, Processing and piezoelectric properties of lead-free (K,Na)(Nb,-Ta)O_3 ceramics, J. Am. Ceram. Soc. 88 (2005) 1190–1196.

[8] J.G. Wu, D.Q. Xiao, Y.Y. Wang, J.G. Zhu, L. Wu, Y.H. Jiang, Effects of K/Na ratio on the phase structure and electrical properties of $(K_xNa_{0.96-x}Li_{0.04})(Nb_{0.91}Ta_{0.05}Sb_{0.04})O_3$ lead-free ceramics, Appl. Phys. Lett. 91 (2007) 252907-1–252907-3.

[9] R.Z. Zuo, X.S. Fang, C. Ye, Phase structures and electrical properties of new lead free $(Na_{0.5}K_{0.5})NbO_3$–$(Bi_{0.5}Na_{0.5})TiO_3$ ceramics, Appl. Phys. Lett. 90 (2007) 092904-1–092904-3.

[10] H.L. Du, W.C. Zhou, F. Luo, D.M. Zhu, S.B. Qu, Z.B. Pei, Perovskite lithium and bismuth modified potassium–sodium niobium lead-free ceramics for high temperature applications, Appl. Phys. Lett. 91 (2007) 182909-1–182909-3.

[11] J. Rödel, W. Jo, K. Seifert, E.-M. Anton, T. Granzow, Perspective on the development of lead-free piezoceramics, J. Am. Ceram. Soc. 92 (2009) 1153–1177.

[12] G.Z. Zang, J.F. Wang, H.C. Chen, W.B. Su, C.M. Wang, P. Qi, B.Q. Ming, J. Du, L.M. Zheng, Perovskite $(Na_{0.5}K_{0.5})_{1-x}(LiSb)_xNb_{1-x}O_3$ lead-free piezoceramics, Appl. Phys. Lett. 88 (2006) 212908-1–212908-3.

[13] J.F. Li, Y. Zhen, B.P. Zhang, L.M. Zhang, K. Wang, Normal sintering of (K, Na)NbO_3-based lead-free piezoelectric ceramics, Ceram. Int. 34 (2008) 783–786.

[14] E.Z. Li, H. Kakemoto, S. Wada, T. Tsurumi, Enhancement of Q_m by co-doping of Li and Cu to potassium sodium niobate lead-free ceramics, IEEE Trans. Ultrason. Ferroelect. Freq. Control 55 (2008) 980–987.

[15] Y. Chang, Z. Yang, L. Wei, Microstructure density and dielectric properties of lead-free $(K_{0.44}Na_{0.52}Li_{0.04})(Nb_{0.96-x}Ta_xSb_{0.04})O_3$ piezoelectric ceramics, J. Am. Ceram. Soc. 90 (2007) 1656–1658.

[16] D.M. Lin, K.W. Kwok, H. Tian, H.W.L. Chan, Phase transitions and electrical properties of $(Na_{1-x}K_x)(Nb_{1-y}Sb_y)O_3$ lead-free piezoelectric ceramics with MnO_2 sintering aid, J. Am. Ceram. Soc. 90 (2007) 1458–1463.

[17] R.P. Wang, H. Bando, M. Itoh, Universality in phase diagram of (K, Na)NbO_3–$MTiO_3$ solid solutions, Appl. Phys. Lett. 95 (2009) 092905-1–092905-3.

[18] C. Ahn, C. Choi, H. Park, S. Nahm, S. Priya, Dielectric and piezoelectric properties of $(1-x)(Na_{0.5}K_{0.5})NbO_3$–$x$$BaTiO_3$ ceramics, J. Mater. Sci. 43 (2008) 6784–6797.

[19] W.J. Wu, D.Q. Xiao, J.G. Wu, J.G. Zhu, B. Zhang, J. Li, Electrical properties and relaxor behavior of $0.995[(K_{0.5}Na_{0.5})_{0.95}Li_{0.05}](Nb_{0.95}Sb_{0.05})O_3$–$0.005BaTiO_3$ lead-free piezoelectric ceramics, in: 2009 18th IEEE International Symposium on the Applications of Ferroelectrics (ISAF), 2009, 4 pp..

[20] H.Y. Park, C.W. Ahn, H.C. Song, J.H. Lee, S. Nahma, K. Uchino, H.G. lee, H.J. Lee, Microstructure and piezoelectric properties of $0.95(Na_{0.5}K_{0.5})NbO_3$–$0.05BaTiO_3$ ceramics, Appl. Phys. Lett. (89) (2006) 062906-1–062906-3.

[21] K. Uchino, S. Nomura, Critical exponents of the dielectric constants in diffused-phase-transition crystals, Ferroelectr. Lett. Sect. 44 (1982) 55–61.

[22] Y.P. Guo, K. Kakimoto, H. Ohsato, Ferroelectric-relaxor behavior of $(Na_{0.5}K_{0.5})NbO_3$-based ceramics, J. Phys. Chem. Solids 65 (2004) 1831–1835.